



Photocatalytic decomposition of pharmaceutical ibuprofen pollutions in water over titania catalyst

J. Choina^a, H. Kosslick^{a,b,*}, Ch. Fischer^b, G.-U. Flechsig^c, L. Frunza^d, A. Schulz^{a,b}

^a University of Rostock, Institute of Chemistry, Department of Inorganic Chemistry, Albert-Einstein-Str. 3a, Rostock, Germany

^b Leibniz Institute of Catalysis e.V. (LIKAT), Albert-Einstein-Str. 29a, Rostock, Germany

^c University of Rostock, Institute of Chemistry, Department of Analytical, Technical and Environmental Chemistry, Dr.-Lorenz-Weg 1, Rostock, Germany

^d National Institute of Materials Physics, Atomistilor Str. 105, P.O. Box MG-7, Bucharest-Magurele, Romania

ARTICLE INFO

Article history:

Received 3 July 2012

Received in revised form

26 September 2012

Accepted 29 September 2012

Available online 8 October 2012

Keywords:

Photocatalytic degradation

Ibuprofen

Pharmaceutical

Titania

Reaction intermediates

Oligomerization

ABSTRACT

Due to the growing importance of low concentrated pollution of surface, ground and drinking, the photocatalytic decomposition of ibuprofen down to low ppm concentrations over titania catalyst has been investigated in detail. The catalyst was characterized by XRD, TEM, diffuse reflection UV-Vis and nitrogen adsorption measurement. The photocatalytic abatement of ibuprofen was monitored by UV-Vis spectrometry, chromatographic by GC/MS, and HPLC coupled electrospray ionization time-of-flight mass spectrometry (ESI-TOF-MS). Catalytic performance has been studied by varying the catalyst and substrate concentration as well as decreasing the catalyst-to-substrate mass ratio over a wide range. The photocatalytic treatment with titania catalyst leads to rapid mineralization of ibuprofen. Formation of intermediate reaction products has been investigated. It is proposed that intermediates in part form oligomeric species, which are responsible for catalyst poisoning. Additional, the influence of the pH value, oxygen supply and catalyst re-use have been checked.

© 2012 Elsevier B.V. All rights reserved.

1. Introduction

Nowadays, about 3000 different compounds are used as medicinal products in human and veterinary health care. They belong to a wide range of different chemical structures. Besides the well-known compounds, the huge number of excreted metabolites (side products) should be considered [1]. The amount of pharmaceuticals and personal care products is equal to the amount of found pesticides.

The extended usage of hazardous pharmaceuticals is accompanied by an increased pollution of surface, ground and drinking water by these substances. However, pollutions occur at low concentration levels. Dramatic impact on ecosystems has been recognized recently. A huge number of pharmaceutical contaminations in lakes and rivers have been already detected [2]. Pharmaceuticals, especially steroids, nonprescription drugs and antibiotics (Table 1) occur in ppb–ppm scale in wastewaters [3]. This number of drugs and their concentrations significant increase each year and achieved in sum concentrations in the ppb to low ppm range.

Besides nonsteroidal anti-inflammatory drugs (NSAID) antibiotics have been widely used for human and veterinary as antibacterial drugs [4]. These pharmaceuticals are excreted by animals and are then released into the aquatic environment. Mainly, they come from fish and animal farms [5,6]. As persistent pollutants, antibiotics and their metabolites have incredible effects on human beings and the aquatic ecological environment. It is generally agreed that aquatic life is most at risk, occurring within drug-contaminated waters. For example, recent British research suggests that estrogen, the female sex hormone, is primarily responsible for deforming reproductive systems of fish.

Many pharmaceutical drug pollutions were also found in drinking water [7,8]. The Environmental Working Group's analyzed of nearly 20 million drinking water samples provided by water suppliers between 2004 and 2009 in U.S. Markedly, they detected 316 contaminants in waters supplied to the public. Nearly two-thirds of these chemicals have been found in the nation's drinking water over the last five years, 201 of them are unregulated [9]. Thus, removal of these dangerous and hazardous contaminations present in low concentration in drinking water is still a challenge.

Ibuprofen (IPB) belongs to a new class of widely used water pollutants, which is biological active and has strong impact on the environment even in small concentrations [10,11]. This compound occurs in unchanged form and incompletely metabolized medicines, which are flushing down toilets by people. Although

* Corresponding author at: Leibniz Institute of Catalysis e.V. (LIKAT), Albert-Einstein-Str. 29a, Rostock, Germany. Tel.: +49 381 4986384; fax: +49 381 4986382.

E-mail address: Hendrik.Kosslick@catalysis.de (H. Kosslick).

Table 1

Frequency detection of pharmaceuticals, hormones and other organic wastewater contaminants in U.S. streams in years 1999–2000 [3].

Percentage of streams with contaminants	Category of contaminants	Representative substances found (median in ppb)
89	Steroids	Cholesterol (0.83), coprostanol (fecal steroid) (0.88)
81	Nonprescription drugs	Acetaminophen (0.11), caffeine (0.081), ibuprofen (0.2), cotinine (nicotine metabolite) (0.05)
74	Insect repellent	DEET (0.06)
66	Disinfectants	Phenol (0.04), triclosan (0.14)
48	Antibiotics	Erythromycin metabolite (0.1), ciprofloxacin (0.02), sulfamethoxazole (0.15)
37	Reproductive hormones	17-alpha-ethynodiol (0.073) (birth control), estrone (0.027)
32	Other prescription drugs	Codeine (0.012), dehydronifedipine (antianginal) (0.012), diltiazem (0.021) (antihypertensive), fluoxetine (0.012) (antidepressant)

by-products of ibuprofen, which are present in the aquatic environment in low concentration are still harmful for human and animals. The occurrence of these side products has been often reported in the literature. However, only high concentrated, polluted solutions were investigated so far [12].

Photocatalytic abatement of hazardous pharmaceuticals by advanced oxidation processes like photocatalysis with titania is of high interest. Especially, there is a lack of knowledge concerning the complete decomposition of low concentrated pollutants and their complete oxidation. Removal of dangerous contaminations like pharmaceuticals, hormones and pesticide from wastewater is still a serious problem [13–15]. So far, only few publications deal with the abatement of these hazardous contaminations [16], moreover most of them still are focused on dyes [17].

The application of titania catalyst is most attractive for effective photocatalytic degradation of drugs and other harmful organic pollutants assisted by UV–Vis radiation [18]. Titania is a nonhazardous compound, which is eco-friendly and does not require any additionally chemicals. In principle, it offers the possibility of complete abatement of drugs and can be recovered and re-used. The analysis of the-state-of-the-art shows that most studies deal with high concentration of pollutants using high catalyst amounts from 0.1 to 1 g/L [19,20] and 10–100 mg/L of substrate [21–23] in order to check catalyst activity or formation by-products. Only few investigations consider the photocatalytic degradation of pharmaceuticals over titania especially at low concentration.

The aim of this work to revisit the catalytic properties of titania in order to get more precise information on catalytic performance of this material at low concentration, which is of increasing importance. The common nonsteroidal anti-inflammatory drug (NSAID) ibuprofen was used as model compound at low concentration in water. The influence of reaction conditions like the catalyst-to-substrate mass ratio, catalyst and ibuprofen concentration was studied in detail. The formation of intermediate reaction products was investigated by ESI-TOF-MS.

2. Experimental

2.1. Materials

Commercially available titania P25 from Degussa Company has been used as photocatalyst. The catalyst was activated in air by heating at 100 °C for 2 h prior to application. The samples were milled in a mortar for photocatalytic use.

Ibuprofen sodium salt (IBP-Na) ($C_{13}H_{17}NaO_2$) was purchased from Sigma–Aldrich. The structure of the used ibuprofen sodium salt model compound is shown in Fig. 1. All solutions used for the photocatalytic experiments were prepared using ultrapure water ($>18 M\Omega$ TOC <2 ppb). Synthetic air with a flow rate of 20 L/h was used to check the influence of additional oxygen supply on the photocatalytic treatment. Additional chemicals: 37 wt.% aqueous solution of hydrochloric acid (Merck, reagent grade 36.5–38.0%),

and sodium hydroxide pellets (J.T. Baker, reagent grade $\geq 97\%$) were used for the pH regulation of the IBP-Na solution.

2.2. Characterization and analyses

The crystallinity and phase composition of the catalyst was checked by powder diffraction measurements carried out on the X-ray diffractometer STADI-P (STOE) using Ni-filtered $Cu K\alpha$ radiation ($\lambda = 1.5418 \text{ \AA}$). The position of the band gap was confirmed by solid state UV–Vis spectrometry in diffuse reflection mode (V-560 Jasco). The catalyst was investigated regarding texture, particle shape and size using transmission electron microscopy, TEM. Prior to TEM measurements, the powdered titania samples were dispersed in ethanol and deposited on copper grids. TEM experiments were done on a LIBRA 120 equipment at 120 kV. Images of samples were recorded with a digital camera with 2000×2000 pixels. The specific surface area and porosity were investigated by nitrogen adsorption–desorption isotherm measurements using a Micromeritics ASAP device.

The concentration of ibuprofen sodium salt was monitored by measuring the absorbance of the samples using a UV–Vis spectrometer (Varian, Cary WinUV). The quantitative progress of the oxidative photocatalytic abatement of IBP-Na was estimated using the calibration plot shown in Fig. 2b. The destruction of the drug was followed by the disappearance of the band corresponding to ibuprofen at 222 nm (Fig. 2a). All data were obtained at room temperature.

The formation and degradation of intermediate products of ibuprofen sodium salt during photocatalytic treatment was checked by ESI-TOF-MS measurements using an electrospray

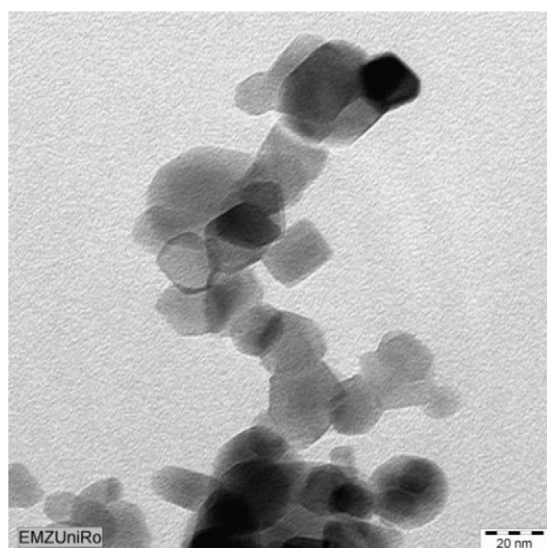


Fig. 1. TEM image of the titania P25 photocatalyst.

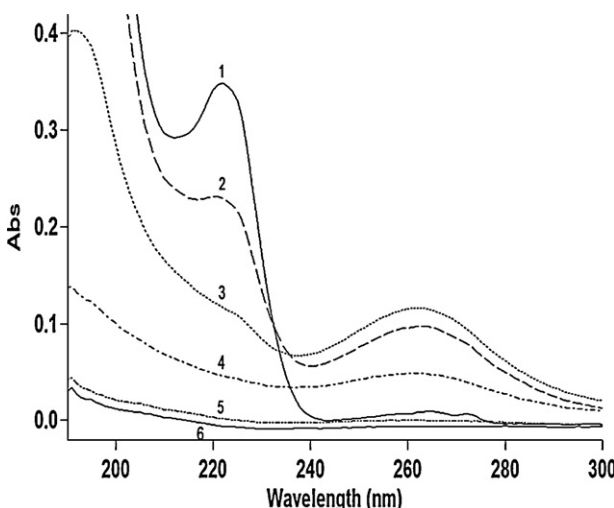


Fig. 2. UV spectra of an aqueous solution of ibuprofen sodium salt after treatment with UV-Vis radiation over P25 photocatalyst, catalyst-to-IBP-Na mass ratio: 4:1, initial concentration of IBP-Na 10 ppm. (1) Starting solution and after (2) 5 min, (3) 30 min, (4) 60 min, (5) 120 min, and (6) 180 min of photocatalytic treatment. Concentration of ibuprofen sodium salt determined based on the absorbance at 222 nm. Formation of temporary products of IBP-Na was followed by the absorbance at 262 nm.

ionization mass spectrometer HPLC System 1200/ESI-TOF-MS 6210 (Agilent). The analysis was carried out in negative electrospray ionization mode. An aqueous solution containing 10 vol.% of methanol (MeOH for HPLC, gradient grade, $\geq 99.8\%$) and 0.1 vol.% formic acid HCOOH was used as mobile phase. The flow rate was 1.0 mL/min. After each photocatalytic run, aliquots of reaction solution were taken for analysis of residual ibuprofen sodium salt by UV-Vis and ESI-TOF-MS. The mass-to-charge range was scanned between m/z 50 and 1000. The GC/MS measurements were carried out in order to identify temporary products formed during photocatalytic treatment (GC/MS System 6890 with MSD 5973 from Agilent).

2.3. Photocatalysis

The photocatalytic treatment of ibuprofen sodium salt (IBP-Na) was carried out in a 250 mL batch reactor. Different amounts of catalyst powder were suspended in the aqueous solution of IBP-Na. The reactor was equipped with 4 UV-Vis solarium lamps (15 W, Philips) irradiating the solution from the top with a total power of 60 W. The radiation intensity of the experimental setup was 3.2 mW/cm². These lamps mainly simulate the UV part of sun light between 320 nm and 400 nm besides of additional emission lines in the visible light range (Fig. 3). The UV intensity is equal to sun light radiation at the Baltic Sea, Rostock, on a clouded day. The radiation intensity was measured using an UV light meter LT Lutron YK-35UV, operating in the spectral range from 290 nm to 390 nm.

The catalyst-to-substrate mass ratio was varied by either changing the substrate concentration at constant catalyst content or changing catalyst content at constant substrate concentration. By this way, the catalyst-to-substrate mass ratio was changed over a wide range of 0.5 and 2. For photocatalytic studies, the aqueous solution containing IBP-Na and the photocatalyst P25 powder was mixed and magnetic stirred during the experiment. The pH value of the solution was adjusted between 3 and 9 by addition HCl and NaOH. The pH values of IBP-Na solution were measured using a pH-meter (WTW pH-330, Germany) equipped with a pH electrode.

Additionally, the oxygen content of the aqueous reaction solution was enhanced by bubbling synthetic air into the solution during the photocatalytic run (flow rate 20 L/h).

Catalyst re-use experiments were carried out by adding aliquots of new IBP-Na solution supplementing the photocatalytic abated amount of this drug. The catalyst was not reactivated for this purpose.

3. Result and discussion

3.1. Photocatalyst

Structural and textural properties of used commercial titania P25 photocatalyst supplied by Evonik have been checked by XRD, TEM and nitrogen adsorption. The XRD data confirm that the high crystalline catalyst consists of a mixture of ca. 80% anatase and 20% rutile. The anatase phase of titania is photocatalytic more active than rutile, however, the band gap of anatase (3.16 eV or 392 nm) is larger than the band gap of rutile (3.0 eV or 413 nm) [24]. The presence of rutile allows the use of a larger spectral range of sun light, because the energy for excitation of electrons from the valence to the conducting band forming electron–holes pairs according to $\text{TiO}_2 + h\nu^{<385 \text{ nm}} \rightarrow e_{cb}^- + h_{vb}^+$ is lower [25].

The UV-Vis diffuse reflectance spectrum of titania P25 shows absorption of UV light of up to ca. 410 nm (Fig. 4) as provided by sunlight and UV-Vis solarium lamps.

The TEM image shows that titania P25 material consists of nano-sized titanium dioxide particles with a primary particle diameter of ca. 10–30 nm. They are regular round shaped and partly aggregated (Fig. 1). The specific surface area of titania is ca. 54 m²/g. The particles itself are not porous as checked by nitrogen adsorption measurements.

3.2. Formation of temporary products

The progress of the photocatalytic abatement of ibuprofen sodium salt over titania P25 was followed by UV-Vis spectroscopy. The starting solution of IBP-Na exhibits two main absorption bands located at 222 nm and 190 nm, which are related to the benzene ring (Fig. 2). After irradiation, the intensity of these bands decreases markedly due to fast photocatalytic oxidation of IBP-Na (Fig. 6a), finally resulting in oxidative ring opening (Fig. 3). It seems that the side group oxidation and oxidative ring opening of the benzene ring of ibuprofen occur simultaneously. Interestingly this is accompanied by the appearance of the new red-shifted band near 262 nm. This strongly indicates the formation of reaction intermediates. This band starts to arise immediately in the first period of photocatalytic treatment (after 5 min), and reaches maximum after 30 min of photocatalytic treatment. It disappears after 180 min indicating complete degradation. Interestingly, with increasing catalyst-to-substrate mass ratio from 2 to 4 (excess of photocatalyst by mass) the formation of temporary reaction products is increased. Obviously, the enhanced amount of catalyst leads to an increase of available very reactive electron–hole pairs at the catalyst surface, which favor the formation of intermediates. The positively charged electron–holes have a high oxidative potential.

Generally, the concentration of temporary reaction products was too small to be detected by GC/MS analysis. Hence, IBP-Na is rapidly abated by the photocatalytic treatment with titania P25 proceeds leaving only small amounts of intermediates.

Electrospray ionization mass spectroscopy (ESI-TOF-MS) has been applied for the identification of temporary products formed during photocatalytic treatment of ibuprofen sodium salt. The ESI-TOF-MS method is sensitive to the formation of the high molecular mass molecules as well as polar species as expected to be formed at oxidative photocatalytic conditions in water (Fig. 3).

The negative ESI-TOF-MS spectrum of the ibuprofen sodium salt starting solution is shown in Fig. 8. The mass-to-charge peak

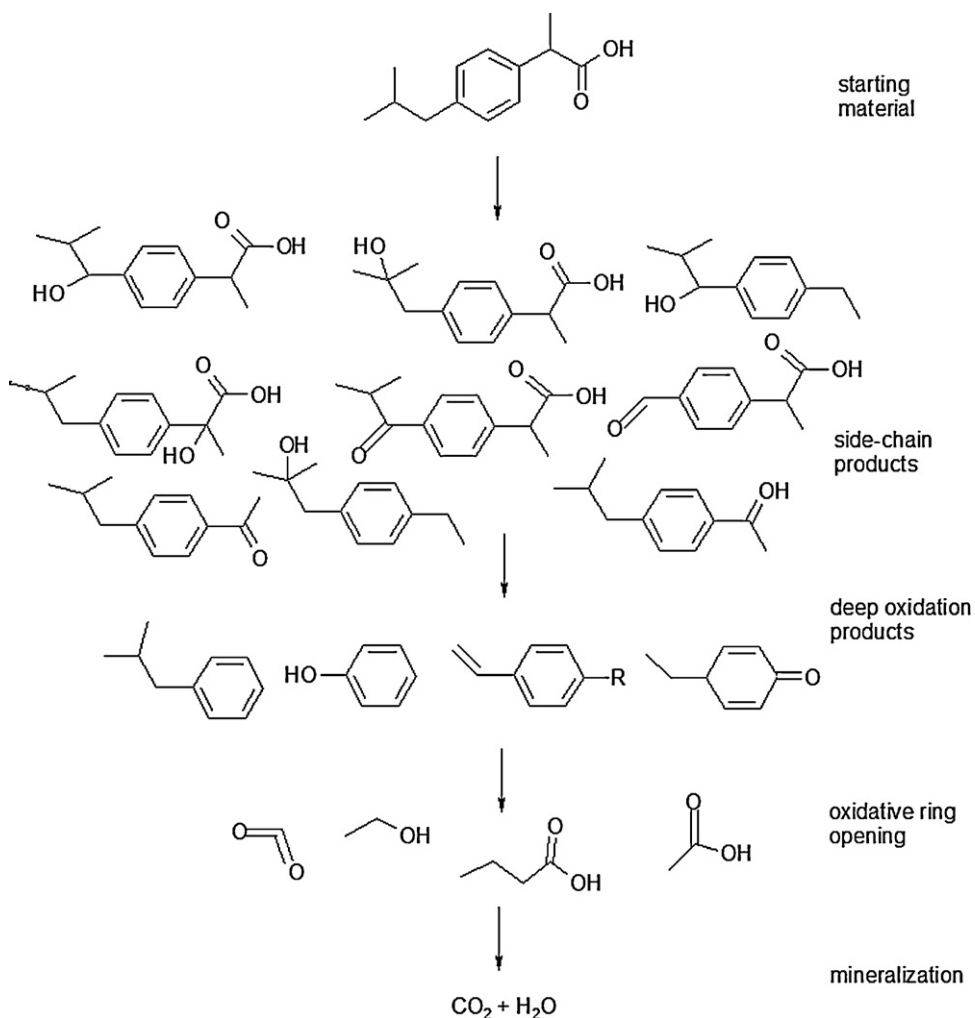


Fig. 3. Formation of side chain products, their deep oxidation products and open ring intermediates of ibuprofen during photocatalytic degradation.

[M-H]⁻ of the IBP anion appears at *m/z* 205. Besides, some lower molecular mass-to-charge peaks are observed belonging to deeper oxidation products (Fig. 3). Additionally, some higher molecular mass peaks at *m/z* 433, 661 and 889 are observed, which could belong to IBP-Na adducts. The equal *m/z* differences between these peaks of 228 correspond to the sum of *m/z* peak 205 plus sodium, the molecular mass of ibuprofen sodium salt. The mass at 273 should belong to an oxidation product of ibuprofen and to corresponding adducts with ibuprofen sodium salt with mass peaks arising at *m/z* 501, 729 and 957.

After 30 min of photocatalytic treatment, MS signals of oligomers products disappear (Fig. 4a). Besides, the ibuprofen anion peak at *m/z* 205 [M-H]⁻, peaks at *m/z* 221, 251, 277, 305, 319 and others appear. Obviously, these higher molecular mass peaks belong to oxidation products of IBP-Na and reaction products of intermediates (Fig. 3). For example, the *m/z* 221 and 251 peaks, which belong to side-chain oxidation products have been identified by Méndez-Arriaga, Ashokkumar and Caviglioli [26–28].

Lower mass [M-H]⁻ peaks arising at *m/z* 175, 146, 133, 129 and lower likely belong to deeper oxidized degradation products like aromatic ketones, carboxylic acids or phenols. At this point, the 262 nm absorbance in the UV-Vis spectrum related to intermediates reaches maximum intensity. Although the concentration of these intermediates is very low (they could not be detected by

GC/MS), the intensity of the corresponding UV absorbance is comparatively high (compare Fig. 2). This finding points to a radical nature of UV detected intermediates.

After 240 min of photocatalytic treatment, the *m/z* 205 peak of the IBP anion disappeared completely. In addition, the intensities of lower *m/z* peaks decreased substantially. Low intense peaks at *m/z* 117 and 129 remained probably belonging to aromatic oxidation products. Interestingly, new peaks of higher molecular mass appear at *m/z* 277 as well as 291 and 305 (Fig. 4b). The mass differences of 14 between these peaks points to methyl substitution. It is proposed that these peaks belong to oligomerization products of aromatics compounds like phenols formed during the photocatalytic decomposition of IBP-Na. These peaks start to arise already after 30 min of photocatalytic treatment.

Green chemistry polymerization and water purification studies with enzymes confirm, that oxygenated aromatics can be radical polymerized [29]. This process is stimulated by low concentrated peroxidases in water at room temperature by reactive oxygen species [30]. Phenols undergo radicalic polymerization to polyphenols as well as C–C bond self-coupling to higher phenols [31,32]. Under strong oxidative conditions, deeper oxidized chinoic intermediates and oligomers are formed [33]. The reaction conditions like low concentration, aqueous solution, pH value range, room temperature as well as active species are similar to photocatalysis with titania. Especially, electron–hole pairs of titania are severe

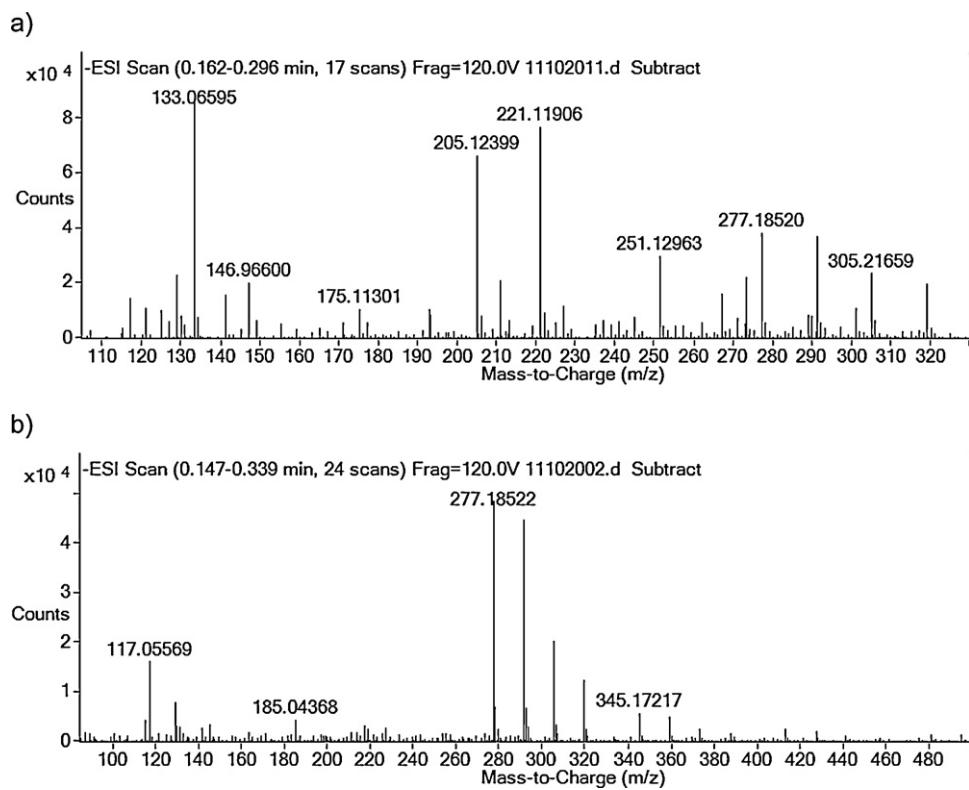
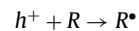
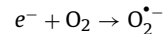
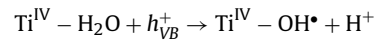


Fig. 4. Negative ESI-TOF-MS of the aqueous IBP-Na solution after photocatalytic treatment over titania P25 catalyst: (a) after 30 min, (b) after 240 min of photocatalysis, IBP-Na conc.: 20 ppm, and cat conc.: 20 mg/L.

oxidants forming superoxide radicals and directly radical reaction products [34,35].



Therefore, it is plausible to assume that similar radical oligomerization reaction occur under photocatalytic conditions as shown in Fig. 5. It is further concluded that the formation of oxygen functionalized aromatics and their polymerization at the surface is most likely the origin of catalyst deactivation by blocking very active sites.

3.3. Abatement of ibuprofen sodium salt and intermediates

The catalytic performance of titania P25 photocatalyst in the abatement of ibuprofen pollutions in water has been investigated in detail. The influence of different reaction conditions such as different substrate and catalyst concentration and corresponding various catalyst-to-substrate mass ratios, pH value and additional oxygen supply on the course of degradation has been investigated. The possibility of catalyst re-use has been checked.

Fig. 6 shows the relative abatement of IBP-Na vs. time for different substrate concentration reaching from 5 to 60 ppm at a catalyst concentration of 10 mg/L during photocatalytic treatment with titania catalyst. The relative abatement (%) of IBP-Na decreases with increasing substrate (IBP-Na) concentration. High relative amounts of IBP-Na are already decomposed in the first 20 min of photocatalytic treatment. Thereafter, the rate of conversion decreases

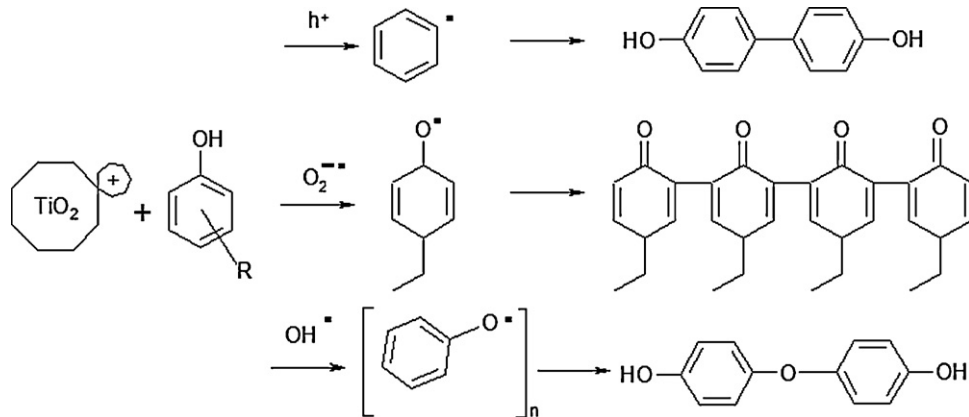


Fig. 5. Possible polymerization of aromatic, phenolic and chinonic intermediates formed by photocatalytic oxidation over titania.

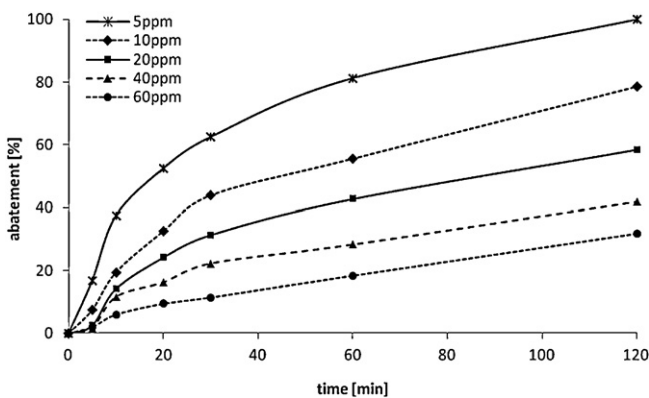


Fig. 6. Relative abatement of ibuprofen sodium salt in water during photocatalytic treatment over P25 photocatalyst using UV-Vis radiation for different IBP-Na conc.: 5, 10, 20, 40 and 60 ppm, cat conc.: 10 mg/L.

distinctly as indicated by the lower slope of the abatement curve above of 30 min of reaction. The diminishment of conversion with photocatalytic treatment time points to a deactivation of the catalyst during the course of reaction. Due to excess of catalyst compared to substrate the relative abatement (Percentage %) of IBP-Na increases with decreasing substrate (IBP-Na) concentrations. However, the absolute abatement shows the reverse tendency. As expected from the concentration dependence of the reaction rate, the absolute amount of abated IBP increases markedly with growing substrate concentration. For example, the percentage removal of IBP after 30 min is 10% (for the 60 ppm solution) and 62% (for the 5 ppm IBP solution), but the absolute amount is 6 mg/L for the 60 ppm solution compared to 3.1 mg/L at 5 ppm.

The effective abatement increases although the relative conversion decreases with growing catalyst loading i.e. increasing substrate concentration (Table 2). This confirms the high catalytic potential of the titania catalyst.

Photocatalytic abatement data observed with IBP-Na over titania are summarized in Table 2. The effective reaction rates of IBP-Na abatement over P25 titania were estimated from experimental data. They show that conversion rates are significantly higher during the first stage (20 min) of photocatalytic treatment than in the second stage of reaction (above 60 min). They differ by a factor of ca. 7.6–2.6 depending on the catalyst loading.

Fig. 7 shows the specific conversion (mg substrate/mg catalyst) of IBP-Na over titania P25 vs. the catalyst-to-substrate (IBP-Na) mass ratio achieved after different times of photocatalytic treatment. As expected, observed specific conversion (mg of IBP-Na per mg of catalyst) increases with longer reaction time, especially at

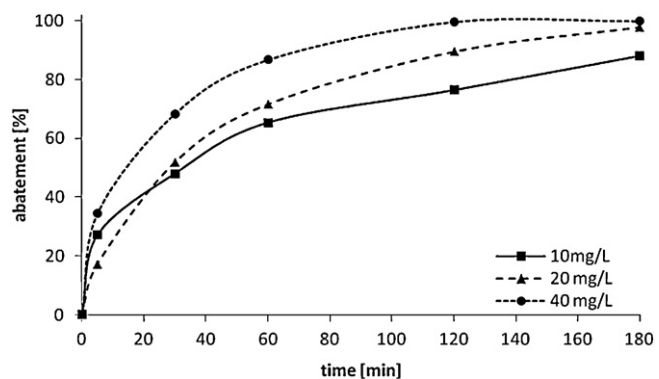


Fig. 8. Abatement of ibuprofen sodium salt in water by P25 photocatalyst under UV-Vis radiation, dependence on cat conc.: 10, 20 and 40 mg/L, IBP-Na conc.: 10 ppm.

low catalyst-to-substrate mass ratio, meaning higher catalyst loading. The conversion depends on the catalyst concentration (amount and strengths of active sites), the adsorption of the substrate on the catalyst surface and the mass transfer. Both, adsorption and mass transfer depend on the substrate concentration. They increase with the concentration gradient. Therefore, the specific conversion increases with decreasing catalyst-to-substrate mass ratio (Fig. 7). At the beginning of the photocatalytic treatment, the most active catalytic sites, the positively charged electron holes, take part in the reaction. This is especially pronounced at high catalyst-to-substrate mass ratio, i.e. excess of catalyst by mass (Fig. 8). Adsorption of the substrate on most active sites is favored under these conditions thereby facilitating photocatalytic conversion.

With growing catalyst amount, meaning excess of catalyst by mass, the efficiency of conversion increases: 10 mg/L < 20 mg/L < 40 mg/L. With catalyst concentration of 10 mg/L ca. 85% of abatement is achieved after 180 min. With increase of the catalyst amount to 20 and 40 mg/L complete abatement is achieved after 180 and 120 min, respectively. Obviously, the activity of the photocatalyst is mainly determined by the most active site, the electron holes under these conditions. In addition, formation of oxygenated radical aromatic intermediates and some polymerization of intermediates to oligomeric or polymeric species occur at the catalyst surface blocking the most active surface sites. Therefore, activity is highest with excess of catalyst and short reaction time. The markedly change of the catalytic performance with reaction time can be explained by the catalyst poisoning. Therefore, activity decreases with prolonging time, especially after the first stage of photocatalytic treatment. The photocatalytic degradation proceeds distinctly slower at prolonged reaction time, because less active sites producing active oxygen species are involved.

Fig. 9 shows the formation of temporary intermediates of IBP-Na during photocatalytic abatement detected by the absorbance at 262 nm in the UV-Vis spectra. Interestingly, the appearance and disappearance of temporary reaction products is closely related to the abatement curves (Fig. 8). Abatement is very fast at the onset of reaction leading to rapid formation of intermediates. Decreasing abatement beyond 30 min of reaction is accompanied by an enhanced abatement of temporary products. They disappear at the same time as IBP-Na is completely abated. This finding additionally confirms that the 262 nm absorbance belongs to reaction intermediates.

3.4. Influence of pH

The pH value of reaction solution may have an important impact on the photocatalytic degradation of organic contaminations

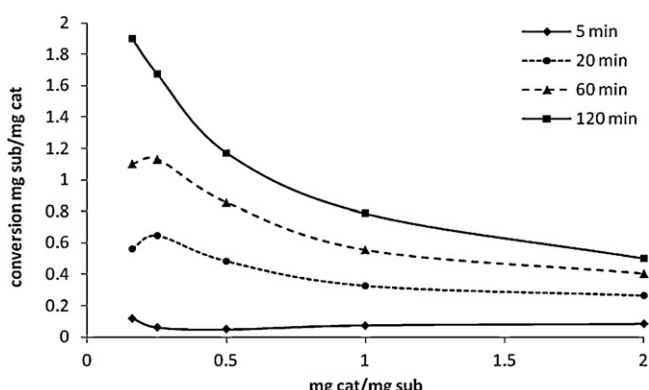


Fig. 7. Specific conversion of IBP-Na in water over titania P25 photocatalyst in dependence on the catalyst-to-substrate mass ratio for different treatment times cat conc.: 10 mg/L.

Table 2

Data of the abatement of ibuprofen sodium salt in water during photocatalytic treatment over titania (cat conc.: 10 mg/L). Abatement (A) and corresponding experimental effective first order reaction rates (r); in the first step (onset of reaction between 0 and 20 min of treatment) and the second step (between 60 and 120 min).

Initial IBP-Na concentration (ppm)	$A_{1\text{st}\text{ step}}$ (mg)	$r_{(1\text{st}\text{ step})}$ (min $^{-1}$)	$A_{2\text{nd}\text{ step}}$ (mg)	$r_{(2\text{nd}\text{ step})}$ (min $^{-1}$)	Rate ratio 1st/2nd step
5	2.6	0.013	1	0.0017	7.6
10	3.2	0.017	2.5	0.004	4.25
20	5.0	0.025	3.5	0.006	4.17
40	5.6	0.028	5.2	0.0087	3.32
60	6.0	0.030	7.8	0.013	2.6

A – mg of IBP-Na. r – mg of IBP-Na per mg of catalyst and minute. R – Ratio of abatement rates of the first and second step.

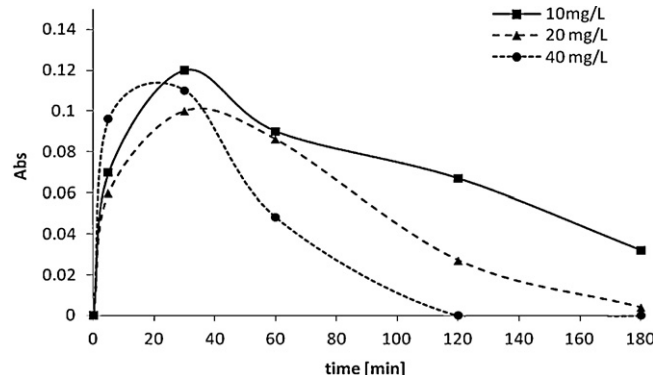


Fig. 9. Formation of temporary products of IBP-Na in water during photocatalytic treatment over titania P25 catalyst based on UV-Vis absorbance at λ_{max} 262 nm for different cat conc.: 10, 20 and 40 mg/L, IBP-Na conc.: 10 ppm.

[36,37]. The surface charge of the catalyst can be changed depending on the chemical nature of the catalyst and its point of zero charge (PZC). In the case of particles with more than one type of surface groups, the surface charge of this material depends on the relative amounts of the different sites. At pH values below the point of zero charge, the catalyst particles are protonated and become positively charged. At higher pH, the surface is deprotonated and more negatively charged.

Fig. 10 shows the influence of the pH on the abatement of IBP-Na vs. time of photocatalytic treatment. In principle, the course of abatement is not changed under acidic or base condition. Rapid abatement of IBP-Na in the first stage of reaction is followed by a slower continuous abatement beyond 60 min of reaction. However, the abatement is diminished compared to neutral reaction condition: neutral > alkaline > acidic solution. This finding can be explained in the following way. The point of zero surface charge of TiO_2 is close to pH 6.8. Ibuprofen is a weak acid with a pK_a value of 4.4. Lower pH will lead to the protonation of titania surface as well as the carboxyl group of ibuprofen. Higher pH increase negative

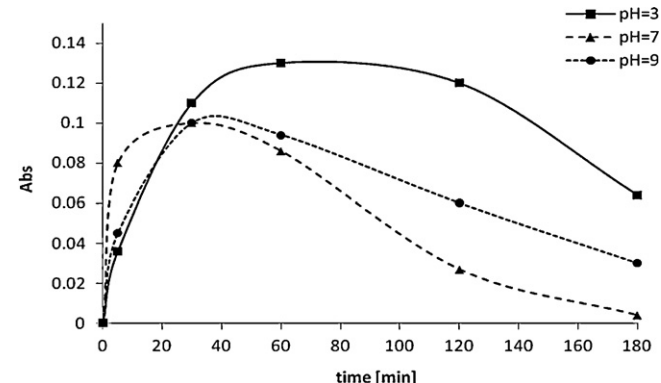


Fig. 11. Influence of pH of the reaction solution on the formation of temporary products of ibuprofen sodium salt during photocatalytic abatement of IBP-Na over P25 catalyst under UV-Vis radiation detected by the change of the absorbance at λ_{max} 262 nm; IBP-Na conc.: 10 ppm, cat conc.: 20 mg/L.

charge of titania surface due to deprotonation of titania and of ibuprofen. Electrostatic repulsion between the substrate and the catalyst surface is increased in both the cases. As a result adsorption of the substrate at the catalyst surface is diminished leading to a decrease of the reaction rate. Protonation proceeds easier under strong acidic conditions than the deprotonation under slightly alkaline conditions (pH 9). Therefore, under both acidic and alkaline condition the abatement of ibuprofen is diminished, compared to the neutral solution. Fig. 11 shows the influence of the pH value of the aqueous reaction solution on the appearance and abatement of temporary products formed during photocatalytic treatment of IBP-Na based on the UV-Vis absorbance at 262 nm. Again, they are closely related to the course of abatement. Intermediates appear immediately with photocatalytic treatment due to high conversion observed at the beginning. Highest formation of temporary products at the onset of reaction is observed under neutral conditions.

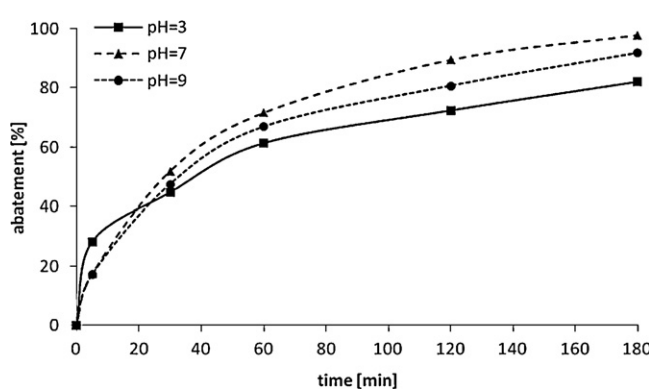


Fig. 10. Influence of pH of the reaction solution on the abatement of ibuprofen sodium salt over P25 catalyst under UV-Vis radiation (IBP-Na conc.: 10 ppm, cat conc.: 20 mg/L).

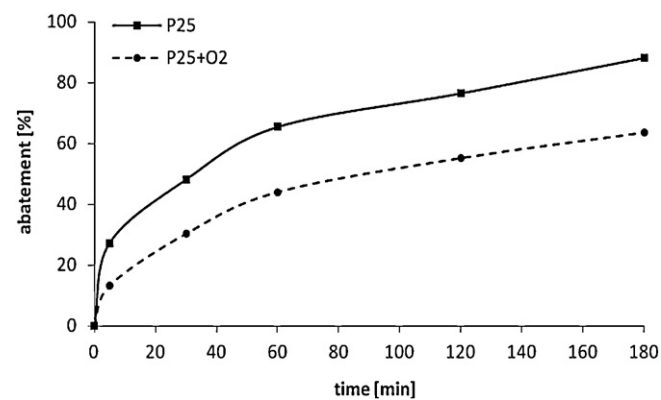


Fig. 12. Photocatalytic abatement of ibuprofen sodium salt over titania P25 catalyst under UV-Vis radiation, influence of additional oxygen supply, IBP-Na conc. 10 ppm, cat conc.: 10 mg/L.

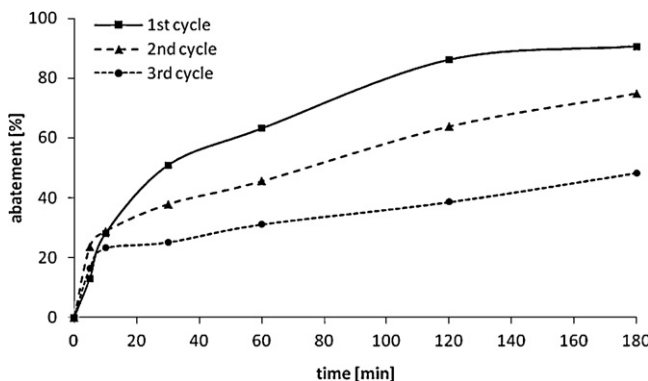


Fig. 13. Photocatalytic abatement of ibuprofen sodium salt in water over titania P25 photocatalyst under UV-Vis radiation after 3 catalyst cycling experiments; IBP-Na conc.: 10 ppm, cat conc.: 10 mg/L.

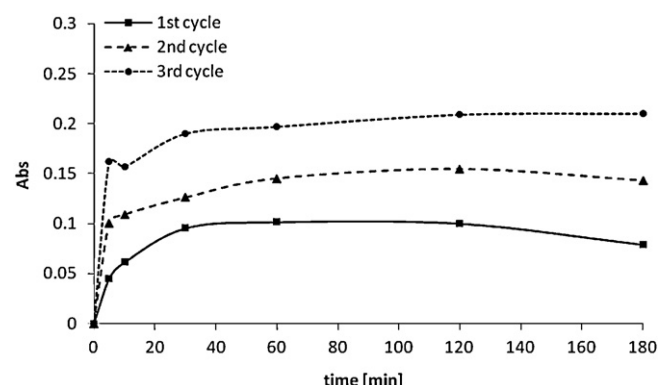


Fig. 14. Formation of temporary products of ibuprofen sodium salt in water during photocatalytic treatment over titania P25 under UV-Vis radiation after 3 catalyst cycling experiments based on the change of the UV-Vis absorbance at $\lambda_{\text{max}} = 262 \text{ nm}$; IBP-Na conc.: 10 ppm, cat conc.: 10 mg/L.

The formation of intermediates is markedly lower under acidic or base conditions. The concentration of intermediates decreases again after reaching maximum at ca. 30 min of reaction. The disappearance of temporary reaction products is closely related to the achieved abatement in this period of time (Fig. 10). They decrease depending on the pH value of the reaction solution in the order: pH 7 > pH 9 > pH 3. This might be due to the more polar character of oxygenated reaction products formed during oxidative decomposition. Electrostatic repulsion is increased compared to the neutral solution.

3.5. Influence of additional oxygen supply

Generally, the supply of additional oxygen is expected to enhance the photocatalytic abatement due to formation of additional super peroxide radicals O_2^{-*} [38,39]. They are formed by the reaction of dissolved oxygen with Ti^{III} surface species trapping conduction band electrons. However, in this case supply of oxygen by bubbling synthetic air into the reaction system did not improve conversion of IBP-Na (Fig. 12). Obviously, the oxygen content achieved by stirring the reaction solution is sufficient high

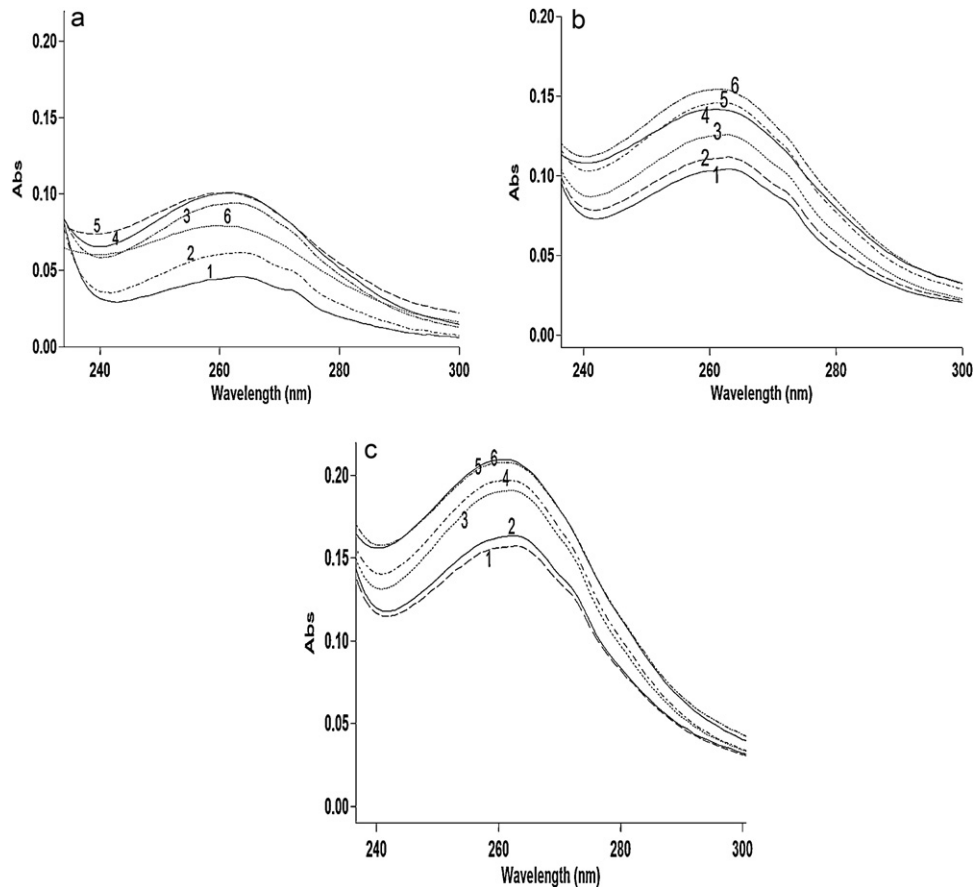


Fig. 15. Formation of temporary products during photocatalytic treatment of ibuprofen sodium salt in water over titania P25 catalyst after re-use experiments. Data based on UV-Vis absorbance by $\lambda_{\text{max}} = 262 \text{ nm}$; IBP-Na conc.: 10 ppm, cat conc.: 10 mg/L. Catalyst cycling experiment: (a) first cycle, (b) second cycle and (c) third cycle. Photocatalytic reaction time: (1) 5, (2) 10, (3) 30, (4) 60, (5) 120, and (6) 180 min.

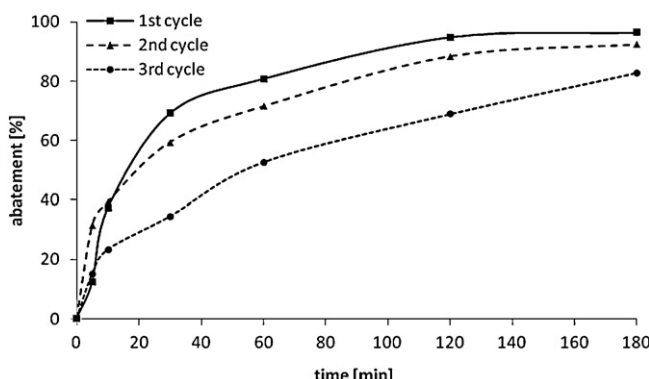


Fig. 16. Photocatalytic abatement of ibuprofen sodium salt in water over titania P25 photocatalyst under UV-Vis radiation after 3 catalyst cycling experiments; IBP-Na conc.: 10 ppm, cat conc.: 20 mg/L.

to maintain the photocatalytic oxidation process at low substrate concentration.

In contrast, conversion decreased. This could be explained by a flotation effect by air bubbles. This effect might be enhanced by the low amount of catalytic material present in aqueous solution. Often a positive effect on the efficiency of photocatalytic conversion has been observed. However, these results were obtained using distinctly larger catalyst amounts of 0.1–1 g catalyst/L, compared to 1–2 mg catalyst/L in this study.

3.6. Re-use of catalyst

The catalyst lifetime is an important economic parameter in photocatalysis [40]. Figs. 13 and 14 show the abatement of ibuprofen sodium salt and formed temporary reaction products over titania during 3 cycles of photocatalytic treatment. Two catalyst-to-substrate mass ratios namely 1:1 and 2:1 have been considered in re-use experiments at constant catalyst concentration. Ca. 90% of IBP-Na has been abated in the first cycle by applying a relative low catalyst-to-substrate mass ratio of 1.1 (catalyst and substrate concentration 10 mg/L). Already in the second cycle, a substantial decrease of the catalyst activity is observed. The abatement of IBP-Na reaches 74% after 180 min of treatment. Finally, in the 3rd cycle the abatement reached only 48% (Fig. 13).

Decreasing catalyst activity with cycling is also reflected in the abatement of intermediates (Fig. 14). The concentration of temporary products immediately increases after starting the photocatalytic treatment. Thereafter, concentration of intermediates is slightly diminished with treatment time. However, concentration of intermediates increases markedly during cycling experiments at a catalyst-to-substrate mass ratio of 1. ESI-TOF-MS data showed formation of oligomeric species from reaction intermediates. Therefore, it is suggested that growing intermediate formation during cycling experiments leads to poisoning of the catalyst by formed oligomers at reactive surface sites. This process is accelerated with cycling due to growing formation and presence of temporary reaction products. Reaction intermediates are then hardly decomposed.

Fig. 15 shows the changes observed with the intensity of the 262 nm absorbance related to reaction intermediates in the UV-Vis spectra of reaction solution after different time of treatment. The spectra belong to the 3 cycling experiments. Clearly, band intensity increases markedly after starting the second and third cycling experiment (Fig. 15b and c) indicating enrichment of intermediates due to incomplete degradation.

Fig. 16 shows the abatement of the ibuprofen sodium salt over P25 photocatalyst assisted by UV-Vis radiation at enhanced photocatalyst-to-substrate mass ratio of 2:1.

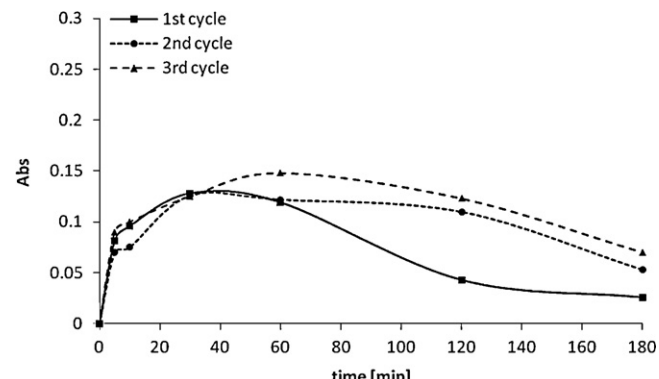


Fig. 17. Formation of temporary products of ibuprofen sodium salt in water under UV-Vis radiation over titania P25 after 3 catalyst cycling experiments based on the change of the UV-Vis absorbance at λ_{max} 262 nm; IBP-Na conc.: 10 ppm, cat conc.: 20 mg/L.

The photocatalytic removal of the IBP-Na from the aqueous solution is significantly enhanced compared to the former used lower catalyst-to-substrate mass ratio of 1:1. After 3 h, 96% of IBP-Na is abated in the first run. It is worth to mention that after the second and third cycle the photocatalytic activity remains high. The degradation of IBP-Na in the second and third cycle achieved still 92% and 82%, respectively.

Again, appearance and abatement of intermediates is closely related to the conversion behavior (Fig. 17). After the appearance at short reaction time, intermediates are abated with prolonged time. This is in contrast to former experiments with lower catalyst concentration. Increased catalyst concentration favors the abatement of intermediates involved in the formation of oligomeric species likely responsible for catalyst poisoning.

4. Conclusion

The photocatalytic results show that the pharmaceutical ibuprofen pollution can be rapidly photocatalytically oxidized over titania P25 catalyst. It is possible to decrease the catalyst concentration in the reaction solution and catalyst-to-substrate mass ratio for markedly savings of catalysts. The actual catalytic performance depends markedly on the choice of reaction conditions. This makes comparison of reported literature data obtained by single testing difficult. The abatement of ibuprofen is accompanied by the formation of temporary reaction products. Reaction intermediates are likely the source of oligomer or polymer formation by radical polymerization leading to catalyst deactivation. The enhancement of the intrinsic photocatalytic activity is of importance and still a challenge.

Acknowledgments

The TEM measurements have been performed by Dipl.-Ing. Gerhard Fulda, Electron Microscopic Centre, Medical Faculty of the University of Rostock, Germany. The authors thank for excellent collaboration. This work was in part supported by the DAAD (German Academic Exchange Service), which is gratefully acknowledged.

References

- [1] T.A. Ternes, Trends in Analytical Chemistry 20 (2001) 419–434.
- [2] U. Jux, R.M. Baginski, H.-G. Arnold, M. Krönke, P.N. Seng, International Journal of Hygiene and Environmental Health 205 (2002) 393–398.
- [3] D.W. Kolpin, E.T. Furlong, M.T. Meyer, E.M. Thurman, S.D. Zaugg, L.B. Barber, H.T. Buxton, Environmental Science and Technology 36 (2002) 1202–1211.
- [4] K. Kümmerer, Chemosphere 45 (2001) 957–969.

[5] J.G. Jones, Water and Environment Journal 4 (1990) 14–18.

[6] G. Rigos, I. Nengas, M. Alexis, G.M. Troisi, Aquatic Toxicology 69 (2004) 281–288.

[7] O.A. Jones, J.N. Lester, Ni. Voulvoulis, Trends Biotechnology 23 (2005) 163–167.

[8] M. Kuster, M.J. López de Alda, M.D. Hernando, M. Petrović, Journal of Hydrology 358 (2008) 112–123.

[9] <http://www.ewg.org/tap-water/reportfindings>

[10] N. Miranda-García, S. Suárez, B. Sánchez, J.M. Coronado, S. Malato, M.I. Maldonado, Applied Catalysis B 103 (2011) 294–301.

[11] N. Klamerth, L. Rizzo, S. Malato, M.I. Maldonado, A. Agüera, A.R. Fernández-Alba, Water Research 44 (2010) 545–554.

[12] F. Méndez-Arriaga, R.A. Torres-Palma, C. Pétrier, S. Esplugas, J. Gimenez, C. Pulgarin, Water Research 42 (2008) 4243–4248.

[13] D.N. Priya, J.M. Modak, P. Trebše, R. Žabar, A.M. Raichur, Journal of Hazardous Materials 195 (2011) 214–222.

[14] J. Mai, W. Sun, L. Xiong, Y. Liu, J. Ni, Chemosphere 73 (2008) 600–606.

[15] Y. Zhang, J.L. Zhou, B. Ning, Water Research 41 (2007) 19–26.

[16] A. Achilleos, E. Hapeshi, N.P. Xekoukoulotakis, D. Mantzavinos, D. Fatta-Kassinos, Separation Science and Technology 45 (2010) 1564–1570.

[17] P. Esparza, M.E. Borges, L. Díaz, M.C. Alvarez-Galván, J.L.G. Fierro, Applied Catalysis A 388 (2010) 7–14.

[18] M. Anpo, P.V. Kama, Environmentally Benign Photocatalysts: Applications of Titanium Oxide-based Materials, Springer, New York, Dordrecht, Heidelberg, London, 2010.

[19] M.M. Haque, M. Muneer, Journal of Hazardous Materials 145 (2007) 51–57.

[20] R. Palomino, M.A. Mondaca, A. Giraldo, G. Penuele, Catalysis Today 144 (2009) 100–105.

[21] F. Méndez-Arriaga, M.I. Maldonado, J. Gimenez, S. Esplugas, S. Malato, Catalysis Today 144 (2009) 112–116.

[22] S. Yurdakal, V. Loddo, V. Augugliaro, H. Berber, G. Palmisano, Catalysis Today 129 (2007) 9–15.

[23] L. Yang, L.E. Yu, M.B. Ray, Water Research 42 (2008) 3480–3488.

[24] R. Vinu, G. Madras, Journal of the Indian Institute of Science 90 (2010) 189–230.

[25] M.R. Hoffmann, S.T. Martin, W. Choi, D.W. Bahnemann, Chemical Reviews 95 (1995) 69–96.

[26] F. Méndez-Arriaga, S. Esplugas, J. Gimenez, Water Research 42 (2008) 585–594.

[27] J. Madhavan, F. Grieser, M. Ashokkumar, Journal of Hazardous Materials 178 (2010) 202–208.

[28] G. Caviglioli, P. Valeria, P. Brunella, C. Sergio, A. Attilia, Journal of Pharmaceutical and Biomedical Analysis 30 (2002) 499–509.

[29] T.J. Collins, C. Walter, Scientific American 294 (2006) 82–90.

[30] L. Frunza, N. Gheorghe, C.P. Ganea, R. Eckelt, H. Kosslick, Reaction Kinetics, Mechanisms, and Catalysis 105 (2012) 195–205.

[31] H.J. Kim, H.S. Kim, International Conference on Biology and Chemistry – IPCBEE 1 (2011) (2010) 105–108.

[32] H. Higashimura, K. Fujisawa, M. Kubota, S. Kobayashi, Journal of Polymer Science Part A: Polymer Chemistry 43 (2005) 1955–1962.

[33] K. Entwistle, D. Tshudy, T.J. Collins, Gordon College, Carnegie Mellon University, personal communication, 2010.

[34] V. Augugliaro, M. Litter, L. Palmisano, J. Soria, Journal of Photochemistry and Photobiology C: Photochemistry Review 7 (2006) 127–144.

[35] S. Žalac, N. Kallay, Journal of Colloid and Interface Science 149 (1992) 233–240.

[36] O.K. Dalrymple, D.H. Yeh, M.A. Trotz, Journal of Chemical Technology and Biotechnology 82 (2007) 121–134.

[37] T. Malygina, S. Preis, J. Kallas, International Journal of Photoenergy 7 (2005) 187–191.

[38] H.P. Shivaraju, International Journal of Environmental Sciences 1 (2011) 911–923.

[39] M. Subramanian, A. Kannan, Korean Journal of Chemical Engineering 25 (2008) 1300–1308.

[40] J. Araña, E.T. Rendón, J.M. Doña Rodríguez, J.A. Herrera Melián, O.G. Díaz, J.P. Peña, Applied Catalysis B 30 (2001) 1–10.